Wind Gust-Induced Flutter of an Elastically Mounted Airfoil: A Fluid-Structure Interaction Study Based on LES

K. Boulbrachene and M. Breuer(✉)

Professur für Strömungsmechanik, Helmut-Schmidt-Universität Hamburg, Hamburg, Germany
{boulbrak,breuer}@hsu-hh.de

1 Introduction

Classical investigations on the aeroelasticity of wings used for the analysis of flutter stability are often carried out based on simplifying model configurations given by elastically mounted rigid wings. For this purpose, either one degree of freedom (1-DOF) considering solely the pitch motion or two degrees of freedom (2-DOF: pitch and heave) are taken into account [5,6]. Concerning the Reynolds number, flows in the transitional regime are of specific interest due to two reasons. First, unmanned air vehicles including Micro Air Vehicles operate in this range. Second, specific flow phenomena such as laminar separation bubbles and transition render this a challenging case. Aeroelastic effects like laminar separation flutter that are different compared to high-Re investigations typically carried out for airplanes are expected. In a precursor study [9] experimental investigations on the fluid-structure interaction (FSI) of a 2-DOF elastically mounted wing were carried out in a wind tunnel. Complementary numerical predictions of the identical coupled FSI setup were performed [4] relying on large-eddy simulations (LES). The results show that coupled high-fidelity solvers allow to predict the FSI problem with an acceptable accuracy leading to either small/large-amplitude oscillations or flutter depending on the case and Re number considered. Note that no wind gusts were taken into account in this preceding study and thus the airfoil had to be initially excited by mechanical perturbations. The objective of the present contribution is to study the aeroelastic response of the same 2-DOF NACA 0012 airfoil in the transitional Reynolds number regime subjected to vertical wind gusts encountered in the atmosphere or the wake of a preceding aircraft. The effect of different gust parameters (gust lengths and amplitudes) on the dynamics of the airfoil is examined. Especially the question of interest is whether certain gusts can induce limit-cycle oscillations or even flutter.

2 Applied Methodology

The numerical methodology applied consists of a partitioned coupled solver combining large-eddy simulations on the fluid side with a solver for the governing equations of the translation and rotation of the rigid wing. The finite-volume Navier-Stokes solver works with curvilinear, block-structured body-fitted grids in the Arbitrary Lagrangian-Eulerian formulation and is second-order accurate in space and time [1]. The standard

© The Author(s), under exclusive license to Springer Nature Switzerland AG 2024
C. Marchioli et al. (Eds.): DLES 2023, ERCO 31, pp. 83–88, 2024.
https://doi.org/10.1007/978-3-031-47028-8_13

Smagorinsky model ($c_s = 0.1$) with van-Driest damping near solid walls is applied. The rigid-body solver receives the fluid forces and moments, and predicts the translational and rotational motions based on Newton's second law using the standard Newmark method of second-order accuracy. The predicted structural displacements of the surface of the airfoil are the input parameters for the adaption of the inner grid. The hybrid grid adaption algorithm (IDW-TFI) developed by Sen et al. [7] is applied. Since in the present application the added-mass effect is negligible, a loose coupling algorithm is preferred. To inject vertical wind gusts into the computational domain, the split velocity method [8] was found to be superior [2] since it is capable of capturing the full interaction between the gust and the structure. Furthermore, the gust can be injected directly in front of the structure, which avoids the strong numerical dissipation associated with regions of coarse grids.

3 Test Case and Setup

As mentioned before, the FSI setup is inspired by precursor investigations [4,9]. The airfoil exposed to a constant free-stream velocity and vertical gravity undergoes heave and pitch motions modeled by a mass-spring-damper system for both DOFs. These are described by six structural parameters: The mass and the mass moment of inertia of the airfoil as well as one material stiffness and one material damping coefficient for each direction of movement; for details refer to [3,4]. In the configuration considered the center of gravity nearly coincides with the center of rotation. In [4,9] this setup was investigated for a wide range of transitional Re numbers. The most interesting case was found to be Re = 33,900, which is employed in the present study. Initiated by external perturbations, a series of sustained large bounded amplitude oscillations was detected in [4,9]. Here, the effect of gust-induced perturbations and their effects on the stability of the airfoil will be examined. For this purpose, vertical gusts which vary solely in the streamwise direction are introduced upstream of the airfoil and convected downstream with the free-stream velocity. Note that a deterministic gust model is applied using an Extreme Coherent Gust (ECG) often denoted "1-cosine" shape defined in the IEC-Standard [10]. In the present study gusts of different wavelengths ($L_g^{x_1}/c$ = 2, 4 and 6) and amplitudes (A_g/u_∞ = 1, 2 and 3) are investigated. Here c denotes the chord length and u_∞ the free-stream velocity.

A C-type grid with about 1.9 million control volumes (CVs) is used and 60 CVs are distributed in the spanwise direction assuming periodic boundary conditions. The grid points are clustered near the surface such that the viscous sublayer can be resolved and no-slip conditions can be applied. At the inlet and the bottom boundary the free-stream velocity is assumed. At the outlet and the top boundary a convective outflow boundary condition is prescribed to assure that the generated vortical structure can leave the computational domain without perceptible disturbances.

4 Results

The aerodynamic forces exerted on the airfoil are compared for the fixed and the elastically mounted airfoil. Figure 1 depicts the lift and pitching moment coefficients of the airfoil encountering a 1-cosine vertical gust with $L_g^{x1}/c = 2$ and $A_g/u_\infty = 2$. Although identical curves are obtained during the airfoil-gust interaction (i.e., until $t^* = t\,u_\infty/c = 3$), the curves of the FSI case continue to oscillate around zero while their CFD counterparts recover to the steady-state values. Oscillating aerodynamic forces contribute to dampening as well as to amplifying the motion as found in [3]. The high-frequency components in the lift and moment coefficients are due to the laminar flow separation taking place at the lower and upper surface of the airfoil.

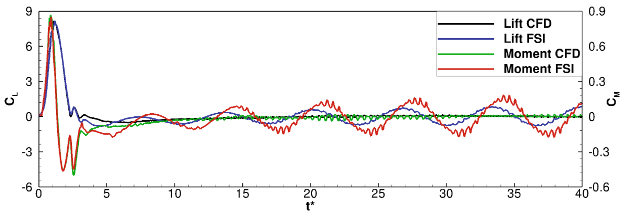

Fig. 1. Instantaneous lift and pitching moment coefficients of the fixed and elastically mounted airfoils subjected to a vertical gust with $L_g^{x1}/c = 2$ and $A_g/u_\infty = 2$.

Figure 2 depicts four instants in time showing the development and transport of flow structures during the airfoil-gust encounter of the elastically mounted wing. Leading-edge vortices are formed and convected downstream when the airfoil undergoes heave and pitch motions as a result of the imposed aerodynamic loads.

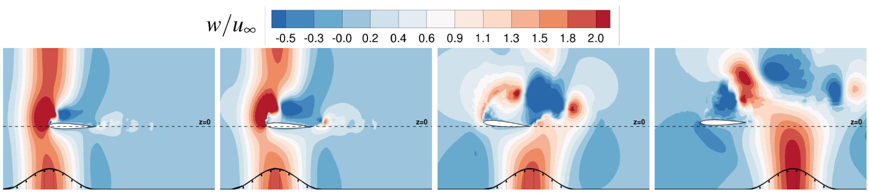

Fig. 2. Snapshots of the total vertical velocity for the elastically mounted airfoil. From left to right: Gust center at leading edge, gust center when lift is maximum, gust center at trailing edge, gust completely left the airfoil.

The aeroelastic response is found to be strongly dependent on the parameters of the gust. Figure 3 shows the instantaneous heave and pitch motion of an airfoil experiencing interaction with a vertical gust of length $L_g^{x1}/c = 4$. For $A_g/u_\infty = 1$ and 2 the amplitudes of both DOFs initially increase upon the gust encounter followed by a steady decrease related to an overall positive damping effect of the aerodynamic forces. Both DOFs are found to eventually settle at a stage in which their amplitudes are sustained and bounded, i.e., a limit-cycle oscillation (LCO) appears. Similar patterns are observed for gusts with $\left(L_g^{x1}/c = 2, A_g/u_\infty = 1,2,3\right)$ and $\left(L_g^{x1}/c = 6, A_g/u_\infty = 1,2\right)$. In contrast, for

$A_g/u_\infty = 3$ gusts with wavelength of $L_g^{x_1}/c \geq 4$ induces significantly larger excitations which trigger a pitch governed diverging motion of the airfoil known as stall flutter (see blue curve in Fig. 3).

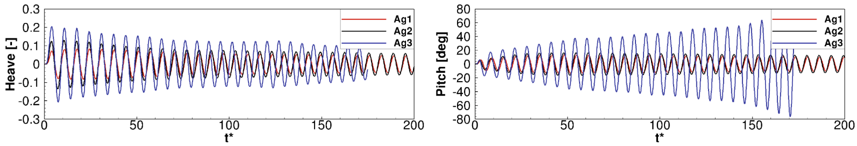

Fig. 3. Instantaneous heave and pitch DOFs when imposing a vertical gust with $L_g^{x_1}/c = 4$ and three different gust strength $A_g/u_\infty = 1, 2$ and 3. (Color figure online)

To investigate the physics involved within a cycle of a limit-cycle oscillation, snapshots of the spanwise y-vorticity ω_y, the skin-friction coefficient C_f, and the location of flow separation are depicted in Fig. 4. When the airfoil starts to pitch up reaching its maximum angle of attack (see Figs. 4a to 4d), the separation starting in the vicinity of the trailing edge moves upstream on the suction side. During the phase when the angle of attack is already decreasing again, vortices are shed from the suction side (see Figs. 4f and 4g). These vortices disappear when the angle of attack tends towards the other extremum (see Fig. 4h) and thus a favorable pressure gradient occurs on the corresponding side of the airfoil. At that stage the same process begins on the lower surface. The laminar separation taking place is mostly two-dimensional and transition to turbulence is detected further downstream justifying the spanwise varying separation line visible in Fig. 4h.

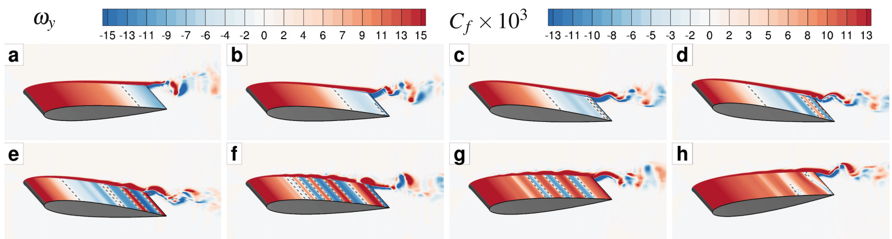

Fig. 4. Normalized y-vorticity ω_y (mid-span slice), skin-friction coefficient C_f (upper surface), and separation location (dashed line) for eight time instants (a-h).

Figure 5 depicts the aerodynamic hysteresis curves of the heave and pitch DOFs upon the interaction with two gusts either with ($L_g^{x_1}/c = 2$, $A_g/u_\infty = 2$) or ($L_g^{x_1}/c = 4$, $A_g/u_\infty = 3$). The former is a LCO case, while the latter is a flutter case. The arrows indicate the direction of advancing time. The black and red circles are used to identify the phases in which energy is being extracted from the flow or delivered to the flow. The direction in which the ellipse is formed indicates the sign of the work done by the aerodynamic coefficients (clockwise positive and counterclockwise negative) [5]. The loops of the two cases can be clearly distinguished. For the first case the clockwise rotation in Fig. 5a signifies positive work of the heave and Fig. 5b points to the overall damping effect of the pitch motion. The total energies shown in Fig. 5c prove that the system undergoes a LCO as the energies of the heave and pitch DOFs cancel out leading to a vanishing total energy of the system. Note that the heave motion is found to be responsible for the energy extraction in the LCO case which is consistent with the outcome of the hysteresis curves.

In contrast, the diverging motion case experiences an increase in the total energy as visible in Fig. 5f. The main part of the energy is extracted by the pitch motion and that continues until the numerical solver can no longer handle the strong deformation of the grid and finally crashes. The hysteresis curves in Figs. 5d and 5e do not have a single turning direction but have a clockwise middle loop and counterclockwise end loops instead. This points to the alternating role that the flow plays in supplying and dampening the energy of the system within a single cycle.

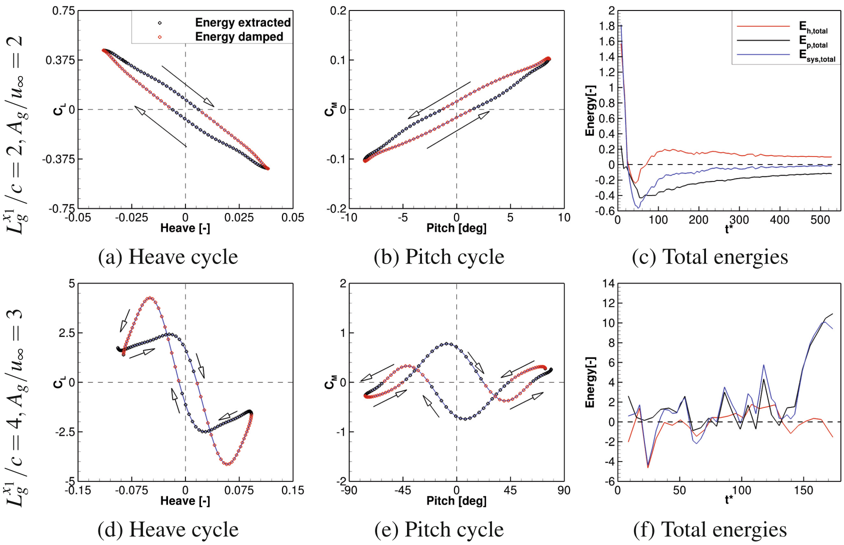

Fig. 5. (a), (b), (d), (e) Aerodynamic hysteresis curves within a single cycle. (c), (f) Instantaneous dimensionless energies of the system.

5 Conclusions

The split velocity method is integrated into a partitioned FSI solver to study the gust-induced oscillations of an elastically mounted 2-DOFs NACA 0012 airfoil. Within a transitional Reynolds number regime, the effect of gust length and strength on the aeroelastic response of the airfoil is investigated. For the same gust width, the initial heave excitation is found to be strongly dependent on the gust strength while that of the pitch showed no dependency. For the same gust strength, wider gusts lead to higher amplitudes in the aerodynamic coefficients and the degrees of freedom. Seven out of nine investigated cases went into a limit-cycle oscillation driven by the laminar separation taking place on the upper and lower surfaces of the airfoil. Two cases excited the airfoil to levels beyond its critical angle of attack and led to a diverging pitch motion. An energy analysis of the coupled system showed that in the LCO case, the heave DOF extracts energy from the flow sustaining the bounded motion of the system. In contrast, in the flutter scenario the energy is accumulatively fed from the flow into the system by the pitch DOF. For further results refer to [3].

Acknowledgements. The project is financially supported by the *German Research Foundation (Deutsche Forschungsgemeinschaft)* under the contract number BR 1847/17-1.

References

1. Breuer, M., De Nayer, G., Münsch, M., Gallinger, T., Wüchner, R.: Fluid-structure interaction using a partitioned semi-implicit predictor-corrector coupling scheme for the application of large-eddy simulation. J. Fluids Struct. **29**, 107–130 (2012)
2. Boulbrachene, K., De Nayer, G., Breuer, M.: Assessment of two wind gust injection methods: field velocity vs. split velocity method. J. Wind Eng. Ind. Aerodyn. **218**, 104790 (2021)
3. Boulbrachene, K., Breuer, M.: Aeroelastic response of an elastically mounted 2-DOF airfoil and its gust-induced oscillations. J. Fluids Struct. **117**, 103828 (2023)
4. De Nayer, G., Breuer, M., Wood, J.N.: Numerical investigations on the dynamic behavior of a 2-DOF airfoil in the transitional Re number regime based on fully coupled simulations relying on an eddy-resolving technique. Int. J. Heat Fluid Flow **85**, 108631 (2020)
5. Poirel, D., Harris, Y., Benaissa, A.: Self-sustained aeroelastic oscillations of a NACA 0012 airfoil at low-to-moderate Reynolds numbers. J. Fluids Struct. **24**, 700–719 (2008)
6. Poirel, D., Métivier, V., Dumas, G.: Computational aeroelastic simulations of self-sustained pitch oscillations of a NACA 0012 at transitional Reynolds numbers. J. Fluids Struct. **27**, 1262–1277 (2011)
7. Sen, S., De Nayer, G., Breuer, M.: A fast and robust hybrid method for block-structured mesh deformation with emphasis on FSI-LES applications. Int. J. Numer. Methods Eng. **111**(3), 273–300 (2017)
8. Wales, C., Jones, D., Gaitonde, A.: Prescribed velocity method for simulation of aerofoil gust responses. J. Aircraft **52**(1), 64–76 (2014)
9. Wood, J.N., Breuer, M., De Nayer, G.: Experimental investigations on the dynamic behavior of a 2-DOF airfoil in the transitional Re number regime based on digital-image correlation measurements. J. Fluids Struct. **96**, 103052 (2020)
10. DIN EN 61400-1:2019, Wind energy generation systems – Part 1: Design requirements. Technical report, IEC (2019)